

# Study of Error based on Six Segments Ring Pair Electrical Resistance Sensor

WANG Xiao-na<sup>1</sup>, DING Yi<sup>1</sup>, SONG Shi-de<sup>2</sup>, HUANG Yi<sup>3</sup>

(1. School of Physics and Optoelectronic Engineering, Dalian University of Technology, Dalian 116024, China; 2. School of Civil Engineering, Dalian University of Technology, Dalian 116024, China; 3. School of Naval Architecture and Ocean Engineering, Dalian University of Technology, Dalian 116024)

## Abstract

There are some defects in the classical theory of ring pair electrical resistance sensor. Aiming at describing the error introduced by the input and output ports, the paper explains the reason, shows the simulation results and gives some suggestions to reduce the error. Then, comparing with the linear arc resistance values, the exact values are calculated using the nonlinear equation. Finally, Considering the temperature difference between the inner and outer walls, the nonlinear result is shown in the follow, and it is consistent with the results of the linear theory, that is, the pipe wall temperature difference does not affect the measurement of corrosion depth.

Keywords: **Corrosion; Ring pair electrical resistance sensor; Error; Resistance measurement**

## 1. Introduction

In recent years, with the depletion of petroleum resources on land, offshore oil exploration and development has gradually started to implement. Under the marine special environmental conditions, the pipeline corrosion monitoring is particularly important. At present, in the field of pipeline corrosion monitoring sensor technology, a variety of new excellent sensors began to be put into use.

Ring pair electrical resistance sensor (RPERS) is a new type of resistance sensor. Compared with the traditional resistance sensor, its inner and outer diameters is consistent with the pipeline, so it can be well integrated into the pipeline system. In addition, As the RPERS has no protrusion in the pipeline, it is conducive to the transport of oil and the operation of the pig. What's more, the sensor is in the same condition with the pipe wall, so the corrosion measurement depth is highly consistent with the corrosion depth of the pipe wall.

Huang Yi<sup>[1]</sup> has successfully developed a set of corrosion monitoring system by using RPERS. Compared with the traditional system, the experimental results have better temperature compensation and can also monitor the local corrosion. However, the arc resistance and the wall temperature distribution use the approximate calculation method, so there may be some theoretical error in the calculation part. This paper focuses on the theoretical error caused by input/output ports and nonlinear effect, some suggestions are shown after simulation experiments.

## 2. Sensor theory

## 2.1 The position and shape of RPERS in pipeline

As shown in Fig.1, the RPERS consists of two metal ring sensors with the same inner diameter and material as the pipeline. The two rings are all coated with chromium oxide except the internal face of corrosion ring. The corrosion ring and the compensation ring are embedded into the pipeline through a connecting ring, which is shown in Fig.1.b. These rings are insulated from neighbor rings by coating of  $\text{Cr}_2\text{O}_3$ , the insulation resistance is higher than  $1\text{M}\Omega$ .

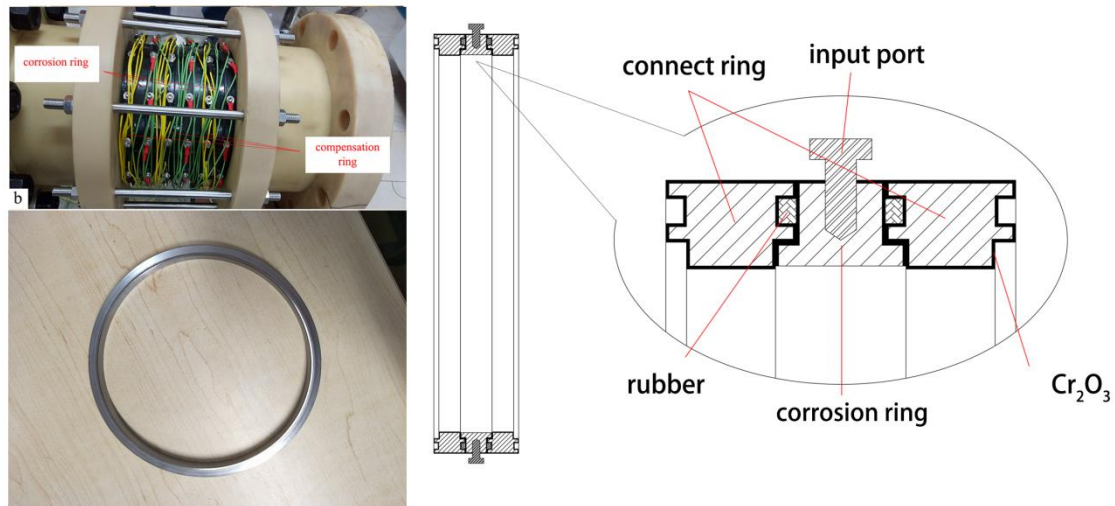


Fig.1 The structure of RPERS

## 2.2 The principle of Kelvin four-wire method (KFWM)<sup>[2]</sup>

Micro-resistance is generally measured by KFWM to reduce the impact of wire resistance and contact resistance<sup>[3]</sup>. as shown in Fig.2, the traditional RPERS corrosion monitoring system using a similar KFWM to measure the resistance.

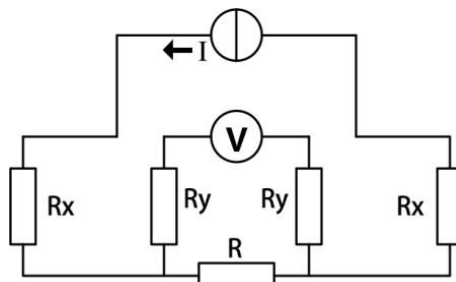


Fig.2 The schematic diagram of KFWM

In Fig. 2,  $R_x$  and  $R_y$  are the sum of the wire resistance and the contact resistance of each branch. Since  $R$  is a micro-resistance, the voltage drop and current through  $R_y$  can be ignored, the current  $I_R \approx I$ , and the voltmeter value  $U_v \approx U_R$ . By Ohm's law.

$$R = \frac{U_v}{I} \quad (1)$$

### 2.3 The measurement principle of RPERS<sup>[4]</sup>

When  $I_1$  is injected as the red path, the voltage value across the segment 2, 3, 5 and 6 in corrosion ring can be measured by using micro ohm meter RM3545. Segment 2 and 3 have the same current, so the resistance ratio  $R_2:R_3$  can be obtained. The segment 5 and 6 have the same current, so the resistance ratio  $R_5:R_6$  can be obtained too. In compensation ring, the resistance ratio  $r_2:r_3$ ,  $r_5:r_6$  can be obtained in the same way. Similarly, when  $I_2$  is injected as the black path, the resistance ratio  $R_3:R_4$ ,  $R_1:R_6$ ,  $r_3:r_4$  and  $r_1:r_6$  can be calculated. When  $I_3$  is injected as the blue path, the resistance ratio  $R_4:R_5$ ,  $r_4:r_5$ ,  $R_1:R_2$  and  $r_1:r_2$  can be calculated. Finally, calculated from the measurement value above, the resistance ratio  $R_i:R_k$  and  $r_i:r_k$  between the random segments in each ring can be obtained, where  $i=1,2,\dots,6$ ,  $k=1,2,\dots,6$ . The corrosion ring and the compensation ring are connected in series, so their total current is equal,  $I_1$  can be expressed as:

$$\frac{U_2}{R_2} + \frac{U_6}{R_6} = \frac{u_2}{r_2} + \frac{u_6}{r_6} = I_1 \quad (2)$$

where  $U_2$ ,  $U_6$  represent the voltage value of segment 2, segment 6 in corrosion ring, and  $u_2$ ,  $u_6$  represent the voltage value of segment 2, segment 6 in compensation ring. In summary, it is easy to get the resistance ratio  $R_i: r_i$  between the corresponding segments of the two rings.

The cross-section parameter of RPERS is shown in Fig.3.

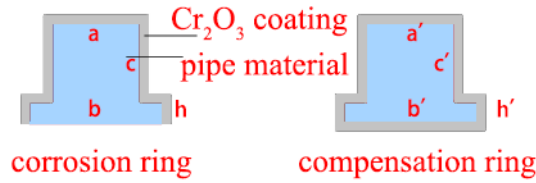


Fig.3 Cross-section parameter

If the inner diameter is much larger than the difference between the inner and outer diameters, Arc resistors can be approximately treated as linear resistors. According to the Fig.3, the resistance  $R_i$  and  $r_i$  can be expressed as:

$$R_i = \frac{L_i \rho(T)}{a_i c_i + b_i h_i} \quad (3)$$

$$r_i = \frac{L'_i \rho(T)}{a'_i c'_i + b'_i h'_i} \quad (4)$$

Where  $L_i$  and  $L'_i$  represent length of the materials,  $\rho(T)$  represent resistivity. The corrosion ring and the compensation ring have the same  $\rho(T)$ , if there is no corrosion, the resistance ratio between the corresponding segments of the two rings can be expressed as:

$$\frac{R_i}{r_i} = \frac{L_i}{L'_i} \times \frac{a'_i c'_i + b'_i h'_i}{a_i c_i + b_i h_i} \quad (5)$$

If the corrosion depth is  $\Delta h_i$ , the resistance ratio can be expressed as:

$$\frac{R'_i}{r'_i} = \frac{L_i}{L'_i} \times \frac{a'_i c'_i + b'_i h'_i}{a_i c_i + b_i (h_i - \Delta h_i)} \quad (6)$$

Combining Eqs.(5),(6), the relation between the corrosion depth and the resistance value can be obtained:

$$\Delta h_i = \left( \frac{a_i c_i}{b_i} + h_i \right) \left( 1 - \frac{R_i r'_i}{r_i R'_i} \right) \quad (7)$$

### 3. Theoretical error analysis

#### 3.1 The error caused by input and output ports.

As shown in Fig.4, the resistance of the RPERs is measured by the KFWM to calculate the resistance ratio of each segment. In actual operation, the current flows from the port a to the port d. the potential of the surface C and surface B can be substituted by the potential of the port c and port b, only if the surface B and C are equipotential surfaces.

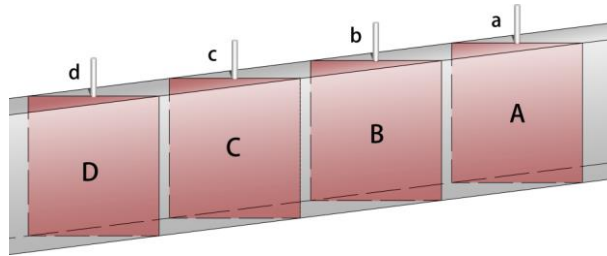


Fig.4 KFWM in actual operation

As shown in Fig.5, the current flows into the port a is approximately the point current flows into the half infinite plane, so the equipotential surfaces close to the port are hemispherical.

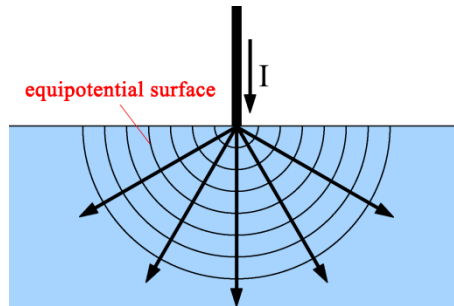


Fig.5 The equipotential surfaces close to the port

Thus, when the cross section B is too close to the cross section A, the cross section B will

be affected by the port A and become a non-equipotential surface, which will introduce the error of the potential measurement.

### 3.2 The error caused by resistance calculation

For the traditional RPERs, when the inside diameter of the sensor is much larger than the difference between the inside and outside diameter, the theoretical calculation of the resistance value is approximately calculated by using the linear resistance Eq.8. The relationship between L and R is linear.

$$R = \rho \frac{L}{S} \quad (8)$$

At present, the ratio between the ring inner diameter and the sensor thickness is generally about 10:1 or at the same order of magnitude, so the theoretical calculation error of the resistance is not negligible, i.e. the relationship between L and R is no longer linear.

#### 3.2.1 Theoretical calculation of arc resistance<sup>[5-6]</sup>

According to the classical physics theory, the arc resistance is calculated by calculus. As shown in Figure.6, the current flows in from the surface A steadily and flows out from the surface B.

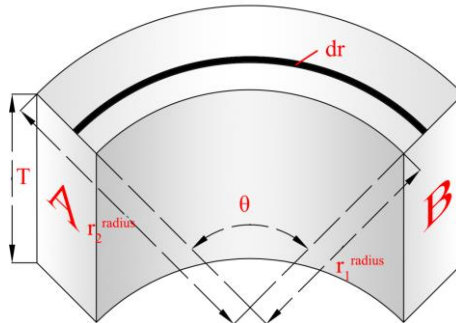


Fig.6 Resistor parameter diagram

In the picture above, the resistance value  $dR$  can be calculated as

$$dR = \rho \frac{\theta r}{T dr} \quad (9)$$

$dR$  is connected with each other in parallel, so  $R$  can be calculated as

$$R = \frac{1}{\int_{r_1}^{r_2} \frac{T dr}{\rho \theta r}} = \frac{\rho \theta}{T \ln \left( \frac{r_2}{r_1} \right)} \quad (10)$$

As shown in Fig.3, after substituting the geometric parameter, the resistance value of segment i can be calculated as

$$R_i = \frac{\rho\theta_i}{b_i \ln\left(\frac{r_f^{\text{radius}} + h_i}{r_f^{\text{radius}}}\right) + a_i \ln\left(\frac{r_f^{\text{radius}} + h_i + c_i}{r_f^{\text{radius}} + h_i}\right)} \quad (11)$$

where  $r_f^{\text{radius}}$  represent the inner diameter of RPERS. Let  $\frac{R_i r_i'}{r_i R_i'}$  be  $M_i$ , according to the Eqs.5,6,7,11. The relationship between  $M_i$  and  $\Delta h_i$  can be calculated as

$$M_i = \frac{b_i \ln\left(\frac{r_f^{\text{radius}} + h_i}{r_f^{\text{radius}} + \Delta h_i}\right) + a_i \ln\left(\frac{r_f^{\text{radius}} + h_i + c_i}{r_f^{\text{radius}} + h_i}\right)}{b_i \ln\left(\frac{r_f^{\text{radius}} + h_i}{r_f^{\text{radius}}}\right) + a_i \ln\left(\frac{r_f^{\text{radius}} + h_i + c_i}{r_f^{\text{radius}} + h_i}\right)} \quad (12)$$

Combining Eqs.7 and Eqs.12, the non-linear relationship between  $M_i$  and  $\Delta h_i$  can be obtained, which is shown in Fig.7,8.

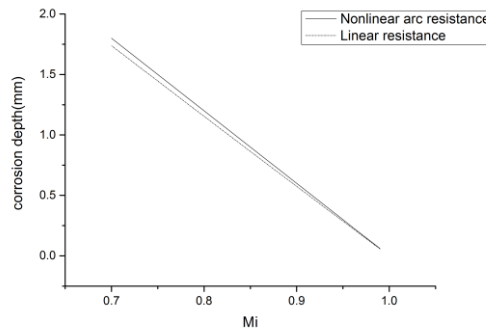


Fig.7 Relationship between linear theory and nonlinear theory

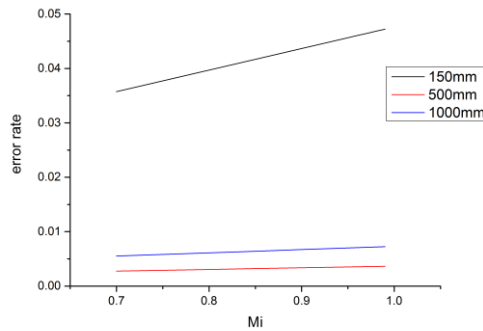


Fig.8 The error rate under different inner diameter conditions

According to Fig.7,8, it can be seen that the theoretical error of linear computation decreases with the increase of  $M_i$ , and the error rate between the linear and the nonlinear theoretical value increase with the increase of  $M_i$ . When the cross section of the RPERS is

constant, the error rate decreases with the increase of the diameter. When the diameter is 150mm, the average error rate reaches about 4%, this theoretical error cannot be ignored. When the diameter increases to 1m and 2m, the average error rate drops to 0.5% and 0.3%, and the error rate decreases slower as the change of  $M_i$  value. In Fig.3, Limited by the shape of the ring cross section, the range of  $\Delta h_i$  is from 0mm to 2mm. In this range, the nonlinear curve approximately shows a straight line. In order to reduce the calculation in the actual operation, the nonlinear curve can be approximately calculated as a linear line.

### 3.2.2 Influence of temperature difference between inner and outer pipe wall on ring resistance measurement.

When the arc resistance is approximately treated as linear resistance, the temperature distribution between the inner and outer pipe wall is linear, and the influence on the calculation of the corrosion depth will be counteracted by the compensation ring<sup>[7-8]</sup>. In fact, the temperature distribution in the pipe wall is not linear. according to the Dirichlet boundary condition, it is calculated by the differential equation under cylindrical coordinates<sup>[9]</sup>, the relation between the temperature and the radius can be calculated as

$$t = t_2 - (t_2 - t_1) \frac{\ln\left(\frac{r}{r_1^{\text{radius}}}\right)}{\ln\left(\frac{r_2^{\text{radius}}}{r_1^{\text{radius}}}\right)} \quad (13)$$

Where  $t_2$  represents the temperature of inner pipe wall,  $t_1$  represents the temperature of outer pipe wall,  $r_1^{\text{radius}}$  represents the inner radius,  $r_2^{\text{radius}}$  represents the outer radius. The relationship between metal resistivity and temperature is linear, combining Eq.10 and Eq.13, the arc resistance can be written as

$$R = \frac{1}{\int_{r_1}^{r_2} \frac{Tdr}{\rho_0 \theta r \left\{ 1 + \alpha \left[ t_2 - (t_2 - t_1) \frac{\ln\left(\frac{r}{r_1^{\text{radius}}}\right)}{\ln\left(\frac{r_2^{\text{radius}}}{r_1^{\text{radius}}}\right)} \right] \right\}}} \quad (14)$$

Where  $\rho_0$  represents the resistivity of arc resistance material at 0°C,  $\alpha$  represents the resistance coefficient of temperature. Through calculating,  $R$  can be written as

$$R = \frac{\rho_0 \theta \alpha (t_2 - t_1)}{T \ln\left(\frac{r_2^{\text{radius}}}{r_1^{\text{radius}}}\right) \ln\left(\frac{1 + \alpha t_2}{1 + \alpha t_1}\right)} \quad (15)$$

The new  $M_i$  can be calculated by using Eqs.15, and the result is consistent with Eqs.13. So we can come to the conclusion that, theoretically, the temperature difference between inner and outer pipe wall has no influence on the measurement of corrosion depth.

**4. Simulation process and results**

*4.1 Simulation of error caused by input and output ports.*

In order to investigate the error of potential measurement in the input and output ports of RPERS, finite element analysis software is applied to simulate the process of resistance measurement. The paper only analyses the input port because of the symmetry of the input and output ports. The sensor model is built in the software interface, the length of inner diameter is 150mm, the length of outer diameter is 168mm. As shown in Fig.3, the lengths of a, b, c and h are 8mm, 12mm, 7mm and 2mm respectively. A series of cross sections close to the input port are created to analyse the potential and current density distributions, which is shown in Fig.9.

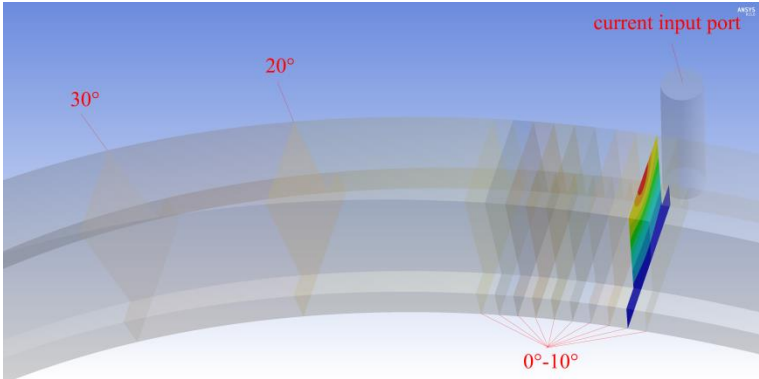


Fig.9 The location of cross sections

The simulation result is shown in Fig.10 and Fig.11.

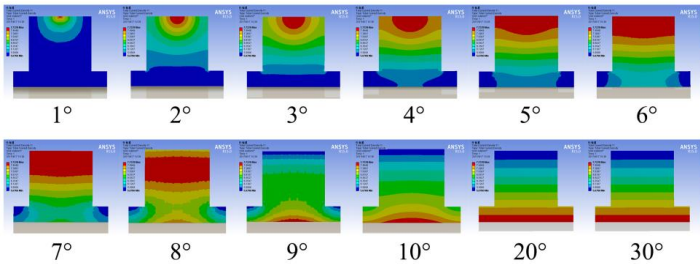


Fig.10 Distribution of current density in each section



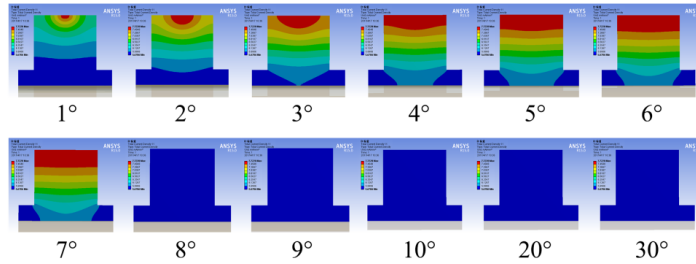


Fig.11 Potential distribution of each section

The simulation results show that, the potential distribution and current density distribution are affected by the input port in varying degrees. The current density distribution is approximately spherical in the cross section 1°, 2°, and 3°. With the increase of the angle between the input port and cross section, the current density gradually becomes more uniform. The location of the maximum current density transforms between the cross section 8° and 9°, the maximum value begins to appear in the bottom section, after 10° the current density distribution tends to stable and shows a gradient distribution map. The potential distribution changes faster than the current density. After cross section 7°, the simulation software is unable to distinguish the potential difference and the faces present equipotential surfaces.

According to the data given by Fig.12, the potential error rate of cross section 1° is about 1.5%, after 8 degrees the error rate between the simulation potential and the theoretical value is less than 0.0349%, which fully meets the requirements of measurement and calculation.

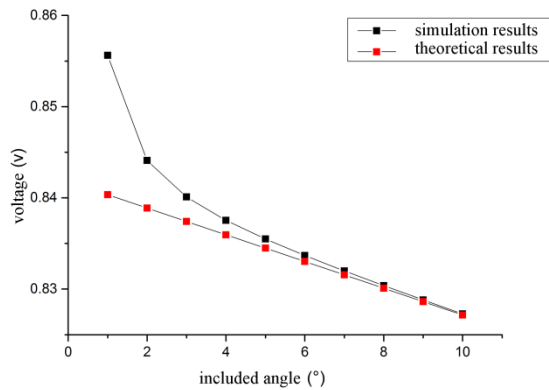


Fig.12 Simulation potential distribution and theoretical potential distribution

#### 4.2 Simulation of error caused by temperature difference between inner and outer pipe wall

The volume parameters of the arc resistor are shown in the Fig.6, the element is made of pipeline steel. The center angle  $\theta$  of the arc is 30°, the inner diameter  $r_1^{\text{radius}}$  is 60mm, the outer diameter  $r_2^{\text{radius}}$  is 110mm, and the thickness  $T$  is 30mm. The inner surface temperature is 200°C. The outer surface temperature is 0°C. All the surfaces except the inner and outer surfaces are set to adiabatic surfaces. The resistivity at 25°C is  $17 \times 10^{-7} \Omega \cdot \text{m}$ , the resistivity temperature coefficient is  $5 \times 10^{-3} \text{R}/^\circ\text{C}$ . The result is shown in the follow.

Table 1

Corrosion depth	The resistance at 25°C	The resistance at 200°C temperature difference	$M_i(25^\circ\text{C})$	$M_i(200^\circ\text{C}$ temperature difference)
0mm	$8.1369 \times 10^{-5} \Omega$	$1.0425 \times 10^{-4} \Omega$	1	1
1mm	$9.9212 \times 10^{-5} \Omega$	$1.2711 \times 10^{-4} \Omega$	0.81962	0.82015
2mm	$1.25950 \times 10^{-4} \Omega$	$1.6139 \times 10^{-4} \Omega$	0.64604	0.64595
3mm	$1.70498 \times 10^{-4} \Omega$	$2.1848 \times 10^{-4} \Omega$	0.47724	0.47716
4 mm	$2.59547 \times 10^{-4} \Omega$	$3.3303 \times 10^{-4} \Omega$	0.31350	0.31303

According to the result we can see that, the different temperature conditions lead to different resistance value, but the  $M_i$  value is identical.

## 5. Conclusions

Through theoretical calculation and simulation analysis, the following conclusions can be drawn:

(1) There is an error in the potential measurement near the current port. In order to reduce the influence, the potential measuring port needs to be away from the current port. the distance departing from the current port is determined by the conductor shape, size and current input mode. The simulation results show that, when the included angle between the current port and the potential measuring port is larger than  $8^\circ$ , the error is negligible, so in the classic RPERS theory included angle between the two ports is  $30^\circ$ , which fully meet the requirements of the engineering calculation.

(2) When the difference between the inner and outer diameter is far less than the inner diameter, the arc resistor can be treated as linear resistor, otherwise the error between the linear and arc resistance cannot be ignored. Based on the same cross section, the error rate increases with the inner diameter. When the temperature difference between the inner and outer pipeline walls exists, the linear and nonlinear calculation show consistent results, that is, the temperature difference between the inner and outer pipeline walls does not affect the measurement of corrosion depth.

## References

- [1] Yunze Xu, Yi Huang, Xiaona Wang, Xuanqin Lin. Experimental study on pipeline internal corrosion based on a new kind of electrical resistance sensor[J]. Sensors and Actuators B: Chemical, 2016,224:37-47.
- [2] Dai Shengyue. The advantages and disadvantages of two wire method and four wire method for measuring resistance. [J]. Science and technology information, 2012 (34): 232-233.
- [3] Zhao Yingwei, Pang Kejian. Test technology and application of Kelvin four wire connection resistance [J].

semiconductor technology, 2005, 30 (11): 43-45.

- [4] HEMBLADE B. Electrical resistance sensor and apparatus for monitoring corrosion : United States, 6946855 B1[P]. 2005-09-20.
- [5] Zhang Sanhui, University Physics [M]. Beijing: Tsinghua University press, 2009.
- [6] Ni Tao, Li Changjin. Comparison of half ring resistance calculated by infinitesimal method and mean value method [J]. west china education research 2012 (4): 84-85.
- [7] Xu Guoliang, Wang Xiaomo, Wu Tian Hua, et al. Engineering heat transfer [M]. Beijing: China Electric Power Press, 2005.
- [8] Huang Yi, Xu Yunze, Wang Xiaona, Li Xiaolong, Tu Shan. Research on pipeline internal wall corrosion monitoring technology based on ring pair resistance sensor [J]. Chinese Journal of mechanical engineering, 2015, (24): 15-23.
- [9] Baijing. Calculation and analysis of cylinder wall temperature [J]. Shanxi: Shanxi architecture, 2007 ,33(25):87.